



**Biomaterials
Science**

**Decellularized extracellular matrix derived from
keratinocytes can suppress cellular senescence induced by
replicative and oxidative stresses**

Journal:	<i>Biomaterials Science</i>
Manuscript ID	BM-ART-06-2022-000897.R1
Article Type:	Paper
Date Submitted by the Author:	06-Aug-2022
Complete List of Authors:	Hoshiba, Takashi; Tokyo Metropolitan Industrial Technology Research Institute,

SCHOLARONE™
Manuscripts

ARTICLE

Decellularized extracellular matrix derived from keratinocytes can suppress cellular senescence induced by replicative and oxidative stresses

Received 00th January 20xx,
Accepted 00th January 20xx

Takashi Hoshiba,^{*a}

DOI: 10.1039/x0xx00000x

Cellular senescence is one of the barriers to maintain *in vitro* three-dimensional (3D) epidermal models for long periods. Therefore, a new culture substrate should be developed to suppress keratinocyte senescence to establish an epidermal model. In this study, reconstituted extracellular matrices (ECM) were prepared by culturing keratinocytes at different passages using the decellularization technique. The ECM prepared by decellularization (dECM) supports keratinocyte adhesion and growth. It has also been demonstrated that dECM suppresses keratinocyte senescence by increasing the antioxidant activity. In particular, dECM derived from younger passaged keratinocytes suppresses senescence more significantly than dECM derived from highly passaged keratinocytes. Moreover, dECM derived from younger passaged keratinocytes can suppress keratinocyte senescence during passage culture. Finally, the dECM derived from younger passaged keratinocytes increased *AQP3* gene expression as an indicator of the functions of basal keratinocytes and the *AQP3* expression ability to respond to all-trans retinoic acid. The dECM derived from younger passaged keratinocytes could be a useful culture substrate for developing an *in vitro* epidermal model.

Introduction

In vitro three-dimensional (3D) epidermal models have been widely used for the safety assessment of chemicals, efficacy testing of cosmetics, and biological studies of skin.^{1,2} Epidermal models are generally prepared by culturing keratinocytes at the air-liquid interface for keratinization. When epidermal models are cultured for a long period, the thickness of the epidermis layer decreases, and its barrier function is weakened.³ These impairments make it difficult to assess the safety and efficacy of long-term chemical and cosmetic treatment. There are several reasons for these impairments in epidermal models after long-term culture. One reason for this is the cellular senescence of keratinocytes in the model. Indeed, senescent keratinocytes are increased in epidermal models after long-term culture.³

Cellular senescence is a state in which cells are viable but non-proliferative, and this state is different from G0 quiescence and terminal differentiation.⁴ Cells undergoing cellular senescence acquire other phenotypes, often leading to functional impairment.^{5,6} For example, the senescence of keratinocytes leads to a delay in their growth and attenuation of basal keratinocyte phenotypes such as aquaporin 3 (*AQP3*, a moisturizing molecule) expression.⁷ In addition, the increase in senescent keratinocytes fails to form thick 3D epidermal models *in vitro*.^{2,3} Therefore, the senescence of keratinocytes should be

suppressed to avoid the impairment of *in vitro* epidermal models after long-term culture.

Keratinocytes adhere to the extracellular matrix (ECM) in the basal layer of the epidermis *in vivo*.⁸ The ECM regulates various cell functions and cell adhesion. For example, the ECM supports cell adhesion and regulates cell growth and differentiation, expression of tissue-specific functions, and responses to soluble factors.^{9,10} The ECM is composed of various proteins and carbohydrates, and their compositions differ among physiological, developmental, and pathological states to precisely and strongly regulate cell functions.^{11,12} Recently, it has been reported that the ECM is remodeled in aged tissues¹³⁻¹⁵, suggesting that cellular senescence is also regulated by the ECM. Therefore, it is expected that the native ECM for non-senescent cells would suppress the senescence of keratinocytes and prevent the impairment of *in vitro* epidermal models after long-term culture.

To reconstitute native ECM *in vitro*, decellularization technique has been widely used.¹⁶⁻¹⁸ Reconstituted ECM by decellularization (decellularized ECM: dECM) is mainly prepared from tissues/organs, and cultured cells.¹⁸ Particularly, cultured cell-derived dECM have been prepared to mimic native ECM in limited regions, such as stem cell niche.¹⁸ Therefore, cultured cell-derived dECM have been used to maintain tissue-specific functions^{19,20} and the stemness of several stem cells during *in vitro* culture.^{21,22} Moreover, it has been reported that mesenchymal stem cell (MSC)-derived dECM can suppress the senescence of MSCs with the maintenance of their stemness.^{23,24} For these reasons, cultured cell-derived dECM have been focused in this study. However, embryonic stem (ES) cell-derived keratinocytes undergo senescence on ES cell-derived

^a 2-4-10 Aomi, Koto-ku, Tokyo, 135-0064, Japan. E-mail: hoshiba.takashi@iri-tokyo.jp

Electronic Supplementary Information (ESI) available: [details of any supplementary information available should be included here]. See DOI: 10.1039/x0xx00000x

fibroblast-derived dECM, although ES cell differentiation into keratinocytes is promoted.²⁵ It is not clear whether dECM can suppress senescence of somatic cells with maintaining tissue-specific functions.

In this study, keratinocyte-derived dECM was prepared and used to suppress the senescence of keratinocytes induced by replicative and oxidative stresses. In addition, I tested whether keratinocytes could increase their epidermal function in the dECM. Two types of dECM were prepared by culturing keratinocytes at different passage numbers (*i.e.*, cellular senescence levels), and their functions were compared. I believe that keratinocyte-derived dECM is useful for developing a new 3D epidermal model with mature epidermal functions and long viability for the safety assessment of chemicals and evaluation of cosmetic efficacy.

Experimental methods

NHEK culture for dECM preparation

Normal human epidermal keratinocytes (NHEKs) at passage 1 were purchased from Lonza (Basel, Switzerland) and were subcultured to passage 3 (P3) and passage 5 (P5) in KGM-Gold keratinocyte growth medium (KGM) on tissue culture polystyrene (TCPS). For the preparation of dECM, P3-NHEKs and P5-NHEKs were seeded on TCPS at densities of 1 and 6×10^4 cells/cm², respectively, and were cultured for 1 week in KGM. The medium was changed every 2-3 days. After culture, decellularization was performed as previously described, with slight modifications.^{26, 27} Briefly, cells were treated with 5 mM EDTA containing phosphate buffered saline (PBS) for 2-3 h at 37°C. After treatment, the samples were washed with PBS twice with gentle pipetting, and then treated with PBS containing 0.5% Triton X-100 and 20 mM NH₄OH for 5 min at 37°C, followed by treatment with PBS containing 100 µg/mL of DNase I and RNase A for 1 h at 37°C. After the treatment, the samples were treated with PBS containing 0.1% glutaraldehyde for 6 h at 4°C. Finally, the samples were treated overnight with PBS containing 0.1 M glycine at 4°C. The prepared dECM were stored at -80°C until use.

To confirm decellularization, cell nuclei and F-actin were labeled with Hoechst33342 and Alexa488-phalloidin as described previously.²⁶ For immunocytochemistry of fibronectin and laminin $\alpha 3$ chain, the samples and bare TCPS were treated with Blocking One (Nacalai Tesque, Kyoto, Japan) for 30 min to block non-specific reactions. After blocking, the samples were treated with primary antibody containing CanGetSignal Immunostain Solution A (ToYoBo, Osaka, Japan) for 2 h at 37°C, followed by treatment with the corresponding secondary antibody conjugated with peroxidase (Dako, Carpinteria, CA) in CanGetSignal immunostain solution B (ToYoBo) for 1 h at 37°C. The primary antibodies used were anti-fibronectin (Santa Cruz Biotechnology, Santa Cruz, CA) and anti-laminin $\alpha 3$ (Abcam, Cambridge, UK). Finally, the labeled proteins were colorimetrically visualized by incubation with 3,3'-diaminobenzidine solution (Dako).

Evaluation of ECM expression pattern

P3- and P5-NHEKs were seeded at a density of 1 and 6×10^4 cells/cm², respectively, and cultured in KGM for 1 week. After culturing, total RNA was isolated using NucleoSpin RNA (Macherey-Nagel, Hoerdet Cedex, France), according to the manufacturer's instructions. Thereafter, cDNA was synthesized by reverse transcription with random hexamers using ReverTra Ace- α (ToYoBo) according to the manufacturer's instructions. Semi-quantitative reverse transcription-polymerase chain reaction (RT-PCR) was performed using BioTaq DNA polymerase (Bioline, London, UK) and specific human primer sets (Table S1). For each experiment, *GAPDH* was amplified to normalize the expression of other genes. PCR products were separated using 1% agarose gel electrophoresis.

Cell adhesion and growth assays

For the cell adhesion assay, P3- and P5-NHEKs were seeded at a density of 1×10^4 cells/cm² and incubated in KGM for 1 h at 37°C. After incubation, the non-adherent cells were removed by washing once with PBS. Adherent cells were fixed overnight with 0.1% glutaraldehyde in PBS at room temperature. Adherent cells were visualized by crystal violet staining and counted in five randomly selected fields using optical microscopy. TCPS was incubated in 2% BSA-containing PBS for 2 h at 37°C, and BSA-coated TCPS was used as a negative control for cell adhesion.

For the cell growth assay, P3- and P5-NHEKs were seeded at a density of 1×10^4 cells/cm² and cultured in KGM for the indicated periods at 37°C. After the culture, dead cells were removed by washing once with PBS, and the cell nuclei were labeled by treatment with 10 µg/mL Hoechst33342 for 5 min. After labeling, the cell nuclei were observed using a fluorescent microscope. The cell nuclei were counted using ImageJ after thresholding.

Cellular senescence evaluation

Cellular senescence was evaluated by senescence associated β -galactosidase (SA- β -Gal) staining and measurement of projected cell areas. For the comparison between P3- and P5-NHEKs, the cells were seeded at a density of 0.35×10^4 cells/cm² and cultured on TCPS for 5 days in KGM. To examine cellular senescence on the dECM under oxidative conditions, P3-NHEKs were seeded at a density of 3×10^4 cells/cm² and cultured in KGM. After 2 days of culture, the cells were treated with 100 nM H₂O₂ containing KGM for 1 day. To examine cellular senescence on the dECM under normal conditions, P5-NHEKs were seeded at a density of 3×10^4 cells/cm² and cultured in KGM for 3 days.

SA- β -Gal staining was performed using a cellular senescence detection kit (SA- β -Gal Staining) (Cell Biolabs, San Diego, CA) according to the manufacturer's instructions. The numbers of SA- β -Gal positive cells and total cells were counted in five randomly selected fields by optical microscopy.

The projected cell areas were measured using the following method: The cells were observed using a phase-contrast

microscope. The projected cell areas were measured using ImageJ after tracing the cell shapes using Photoshop CC and a graphics tablet (Bamboo Fun, Wacom, Saitama, Japan).

Measurement of intracellular reactive oxygen species (ROS) levels

For the measurement under oxidative conditions, P3-NHEKs were seeded at a density of 3×10^4 cells/cm² and cultured in KGM for 2 days. After culturing, the cells were incubated with 80 μ M 2', 7'-dichlorodihydrofluorescein diacetate (H₂DCFDA) in PBS for 45 min at 37°C. After incubation, the cells were washed once with PBS and incubated with 500 μ M H₂O₂ in PBS. After 2 h of incubation, relative fluorescence units (RFU) were measured using a fluorescent microplate reader with excitation/emission at 485 nm/528 nm. For measurement under normal conditions, P5-NHEKs were seeded at a density of 3×10^4 cells/cm² and cultured in KGM for 3 days. After culturing, the RFU was measured using the method described above without H₂O₂ treatment. After RFU measurement, the cells were lysed with 0.5% Triton X-100 solution, and the total protein amounts were measured to normalize RFU with a BCA protein assay kit (ThermoFisher Scientific, Waltham, MA) according to the manufacturer's instructions.

Gene expression analysis by real-time PCR

For the gene expression analysis of antioxidant enzymes, the cells were cultured according to the methods described above. For *AQP3* expression analysis, P3-NHEKs were seeded at a density of 3×10^4 cells/cm² on P3-dECM and TCPS and cultured for 3 days in KGM. After culture, the cells were exposed to all-trans retinoic acid (ATRA) at the indicated concentrations for 3 h. Finally, total RNA was isolated and cDNA was synthesized using the method described above.

Real-time PCR was used to amplify *GAPDH*, *SOD1*, *GPX1*, *CAT*, and *AQP3* using specific primers and probes or TaqMan Gene Expression Assays (Table S2). The reaction was performed with 2.5–10 ng cDNA, 300 nM primers, 150 nM probe (or TaqMan Gene Expression Assays), and Premix Ex Taq (Probe qPCR) (TaKaRa, Shiga, Japan) according to the manufacturer's instructions. Gene expression levels relative to *GAPDH* were calculated using the comparative Ct method.

Passage cultures on P3-dECM

NHEKs at passage 2 or 3 were seeded at a density of 0.67 or 1×10^4 cells/cm² and cultured for 5 days in KGM. After culturing, the cells were harvested by treatment with trypsin/EDTA solution (Lonza) for 5 min. Harvested cells were counted using a hemocytometer. For SA- β -Gal staining, P2-NHEKs were passaged twice on P3-dECM and TCPS. Passaged NHEKs were seeded at a density of 3×10^4 cells/cm² and cultured for 3 days in KGM. After culturing, SA- β -Gal staining was performed as described above.

Statistical analysis

All statistical analyses were performed using R, language, and environment for statistical computing. Statistical differences

among 3 samples were to be determined, the differences were determined by analysis of variance (ANOVA). Tukey's multiple comparison test was applied as a *post hoc* test. Statistical differences between two samples were determined using an unpaired Student's *t*-test.

Results

Preparation of dECM derived from cultured keratinocytes at different passages

In this study, normal human epidermal keratinocytes at passage 3 and 5 (P3-NHEKs and P5-NHEKs) were used to prepare dECM to assess the effects of cellular senescence levels of the original cells for dECM preparation. Cellular senescence levels of these NHEKs were checked by detecting the activity of senescence-associated β -galactosidase (SA- β -Gal), which increases in senescent cells.^{4, 28} The number of SA- β -Gal-positive cells was increased in P5-NHEKs (Figure 1A). The percentages of SA- β -Gal positive cells in P3-NHEKs and P5-NHEKs were $11.2 \pm 1.3\%$ and $43.2 \pm 10.3\%$, respectively. Enlargement of cell size is also a characteristic of senescent cells.²⁸ P5-NHEKs were larger than P3-NHEKs (Figure 1A). These observations indicate that the senescence level of P5-NHEKs was higher than that of P3-NHEKs.

Thereafter, ECM expression patterns were compared between P3-NHEKs and P5-NHEKs using semi-quantitative reverse transcription polymerase chain reaction (RT-PCR) (Figure 1B). Keratinocytes adhere to the basement membrane *in vivo*⁸, and the gene expression levels of major basement membrane components were examined. Few differences were observed in laminin α 3 chain (*LAMA3*), laminin α 5 chain (*LAMA5*), type IV collagen α 1 chain (*COL4A1*), and heparan sulfate proteoglycan 2 (*HSPG2*) (also known as perlecan) gene expression levels between P3-NHEKs and P5-NHEKs. In contrast, nidogen (*NID-1*) gene expression levels decreased in P5-NHEKs, suggesting that the deposited ECM molecules were different between P3-NHEKs and P5-NHEKs.

P3-NHEKs and P5-NHEKs were decellularized to prepare dECM after one week of culture. Decellularization was confirmed by detecting cell nuclei and fibrillar actin (F-actin) (Figure 1C). Evident cell nuclei and F-actin were observed in the samples before decellularization. After decellularization, no evident cell nuclei or F-actin were observed. To confirm whether ECM molecules were retained after decellularization, retained fibronectin (also produced by keratinocytes²⁹) and laminin α 3 chains were detected by immunocytochemistry (Figure 1D). Both ECM proteins were detected in P3-NHEK-derived dECM (P3-dECM) and P5-NHEK-derived dECM (P5-dECM), whereas they were barely detected in bare TCPS. These results suggested that ECM proteins were retained even after decellularization, and P3-dECM and P5-dECM were successfully prepared.

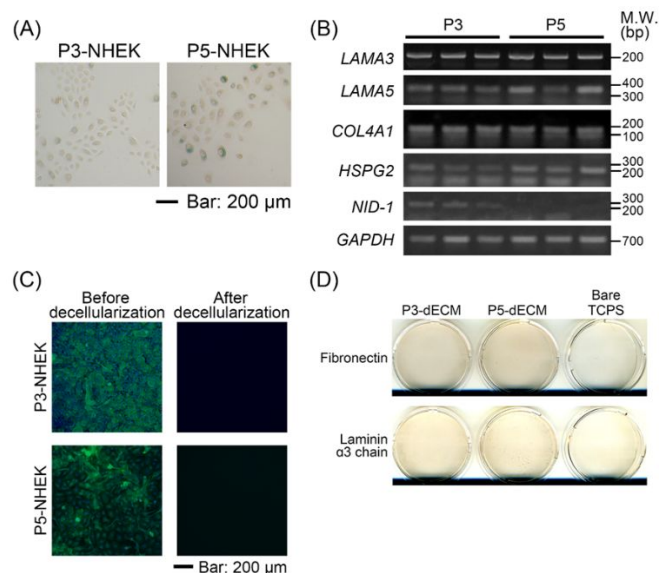


Figure 1. Preparation of NHEK-derived dECM. (A) SA-β-Gal staining of P3- and P5-NHEKs. Bar indicates 200 μm. (B) ECM expression pattern of P3- and P5-NHEKs. (C) Confirmation of decellularization. Blue and green indicate cell nuclei and F-actin, respectively. Bar indicates 200 μm. (D) Immunocytochemistry of fibronectin and laminin-α3 chain.

Cell behaviors on NHEK-derived dECM

Cell behavior was compared between P3-dECM and P5-dECM (Figure 2). First, the adhesion of P3-NHEKs and P5-NHEKs on NHEK-derived dECM was compared after 1 h of incubation (Figure 2A and 2B). The numbers of adherent P3-NHEKs and P5-NHEKs were greater on P3-dECM, P5-dECM, and bare TCPS than that on bovine serum albumin (BSA)-coated TCPS, a negative control for cell adhesion, indicating that NHEK-derived dECM possesses cell adhesion activity. The numbers of adherent P3-NHEK tended to be smaller on P3-dECM than on P5-dECM and TCPS (Figure 2A). Few differences in the numbers of adherent P5-NHEKs were observed among P3-dECM, P5-dECM, and TCPS (Figure 2B).

Second, it was examined whether the cells can be cultured on the prepared dECM. NHEKs can be healthily spreading on P3-dECM, P5-dECM, and bare TCPS after 3 days of culture (Figure 2C). Then, the growth of P3-NHEKs and P5-NHEKs was compared (Figure 2D, 2E, S1, and S2). The numbers of both P3- and P5-NHEKs were in the order of P3-dECM < P5-dECM < TCPS after 7 days of culture (Figure 2D and 2E). However, the growth percentages of P3-NHEKs and P5-NHEKs were in the order of TCPS < P3-dECM ≤ P5-dECM and P3-dECM ≤ TCPS and P5-dECM, respectively (Figure S1 and S2). Therefore, it seemed that the lowest cell numbers on P3-dECM after 7 days culture were due to low initial cell adhesion rather than slow cell growth.

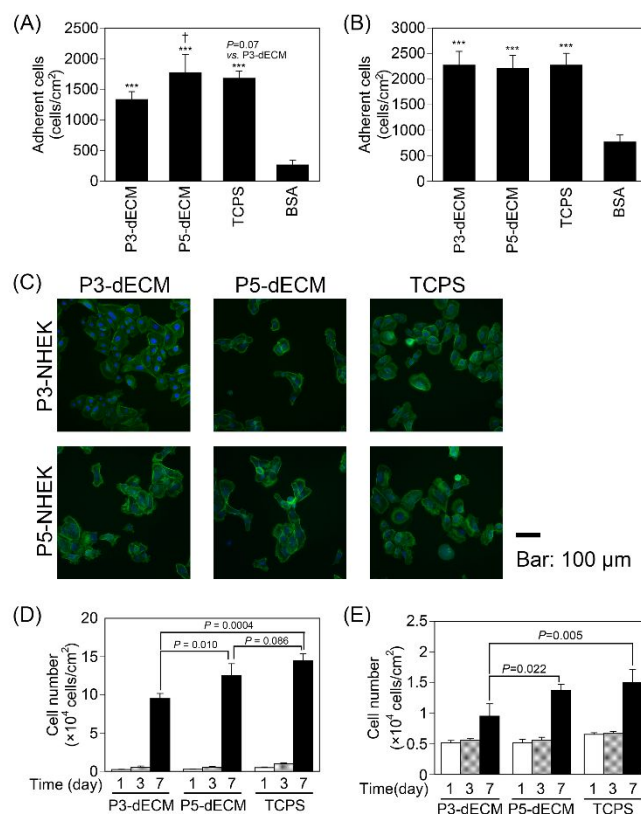


Figure 2. NHEK behavior on NHEK-derived dECM. The adhesion of (A) P3-NHEKs and (B) P5-NHEKs after 1 h. BSA indicates BSA-coated TCPS. Data represent means ± SD (n=4). ***: $P < 0.005$ vs. BSA, †: $P < 0.05$ vs. P3-dECM. (C) NHEK shapes after 3 days of culture. F-actin was stained with Alexa488-conjugated phalloidin. Cell nuclei were counter-stained with Hoechst33342. Scale bar indicates 100 μm. The growth of (D) P3-NHEKs and (E) P5-NHEKs after 1, 3, and 7 days. Data represent means ± SD (n=4).

Cellular senescence of NHEKs was suppressed on dECM

To assess whether cellular senescence was suppressed by dECM, P3-NHEKs were cultured on dECM with oxidative stress to induce cellular senescence. Senescent P5-NHEKs were cultured in dECM without oxidative stress. Cellular senescence was assessed under these conditions (Figure 3A).

P3-NHEK senescence on dECM with oxidative stress.

The percentage of SA-β-Gal-positive cells was measured by SA-β-Gal staining after P3-NHEKs were cultured in the presence of 100 nM H₂O₂ for 1 day (Figure 3B and 3C). The percentage of SA-β-Gal-positive cells decreased by 50% on P3-dECM compared to P5-dECM and TCPS. In addition, the projected cell areas decreased on P3-dECM compared with those on P5-dECM and TCPS (Figure 3D and Table S3). These results indicate that P3-dECM suppressed the senescence of P3-NHEK under oxidative conditions.

P5-NHEK senescence on dECM without oxidative stress.

The percentage of SA-β-Gal-positive cells was measured by SA-β-

Gal staining after P5-NHEKs were cultured in the absence of H_2O_2 (Figure 3E and 3F). The percentage of SA- β -Gal positive cells was in the order of P3-dECM < P5-dECM < TCPS, and decreased by 15% on P3-dECM compared with TCPS. In addition, the projected cell areas decreased on P3-dECM compared with those on P5-dECM and TCPS (Figure 3G and Table S4). These results indicate that P3-dECM suppressed the senescence of P5-NHEKs during culture.

Antioxidant activity of NHEKs increased on dECM

Oxidative stress is a stressor that induces cellular senescence is an oxidative stress.⁴ Therefore, the antioxidant activity of NHEKs on dECM was examined under both oxidative and normal conditions.

Antioxidant activity of P3-NHEKs on dECM with oxidative stress.

Senescence of P3-NHEKs was suppressed on P3-dECM under oxidative conditions. It was hypothesized that antioxidant activity increased on P3-dECM. To test this hypothesis, intracellular ROS levels were measured under oxidative conditions. Intracellular ROS levels decreased by approximately 20% on P3-dECM and P5-dECM compared with TCPS (Figure 4A). Moreover, the gene expression levels of the antioxidant enzymes, superoxide dismutase 1 (*SOD1*) and glutathione peroxidase (*GPX1*), significantly were significantly higher on P3-dECM and P5-dECM than on TCPS (Figure 4C(a) and 4C(b)). The gene expression level of another antioxidant enzyme, catalase (*CAT*), tended to be higher on P3-dECM and P5-dECM than on TCPS (Figure 4C(c)). These results indicate that the antioxidant levels of P3-NHEK increased on P3-dECM and P5-dECM under oxidative conditions.

Basal antioxidant activity of P5-NHEKs on dECM. Senescence of P5-NHEKs was suppressed on P3-dECM under normal conditions. It was hypothesized that basal antioxidant activity increased on P3-dECM. Therefore, basal intracellular ROS levels were measured without H_2O_2 (Figure 4B). Basal intracellular ROS levels decreased by approximately 30% on both P3-dECM and P5-dECM compared to TCPS. Moreover, *GPX1* expression was significantly increased on P3-dECM and P5-dECM compared with TCPS (Figure 4D(b)). *CAT* expression increased only on P5-dECM, but the expression level on P3-dECM was similar to that on TCPS (Figure 4D(c)). No evident differences were observed in *SOD1* expression levels among P3-dECM, P5-dECM, and TCPS (Figure 4D(a)). These results indicate that the basal antioxidant levels of P5-NHEK increased on P3-dECM and P5-dECM under normal conditions.

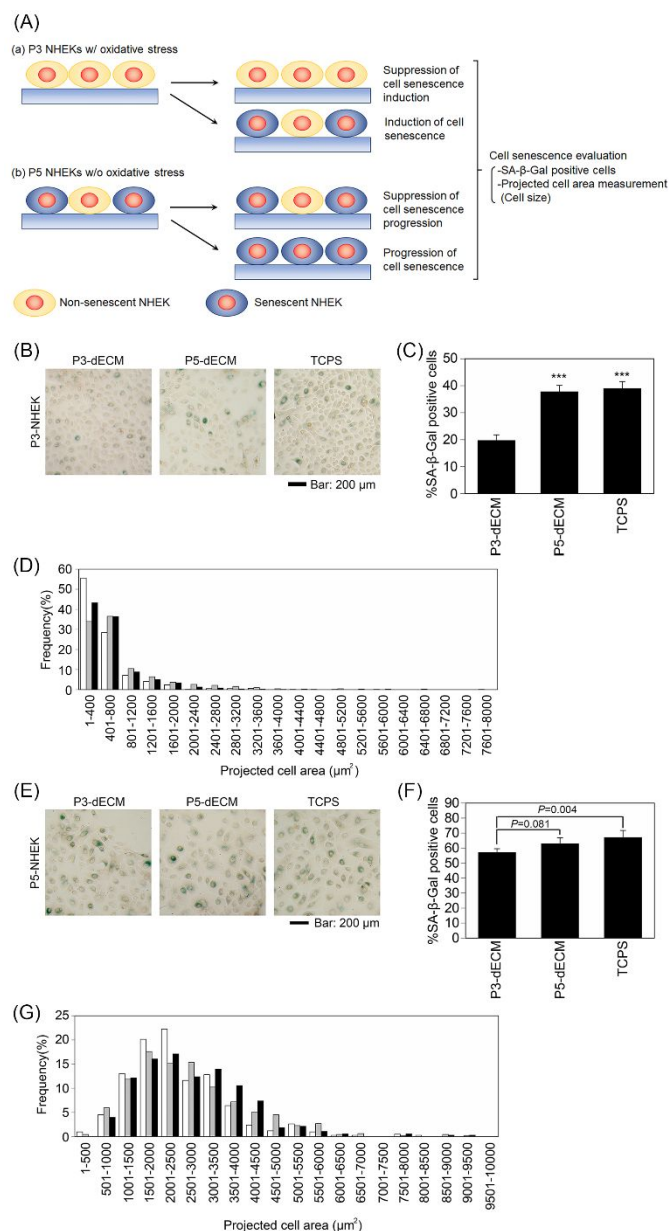


Figure 3. Senescence of NHEKs on dECM. (A) Schematic illustration of cell senescence experiments. (a) Experiments under oxidative condition. (b) Experiments under non-oxidative condition. SA- β -Gal staining of (B) P3-NHEKs under oxidative condition and (E) P5-NHEKs under normal condition. The percentages of SA- β -Gal positive cells of (C) P3-NHEKs under oxidative condition and (F) P5-NHEKs under normal condition. Over 550 cells/sample were measured. Data represent means \pm SD (n=5). Projected cell area of (D) P3-NHEKs under oxidative condition and (G) P5-NHEKs under normal condition. White, gray, and black bars indicate P3-dECM, P5-dECM, and TCPS, respectively. Over 350 cells were measured in each condition.

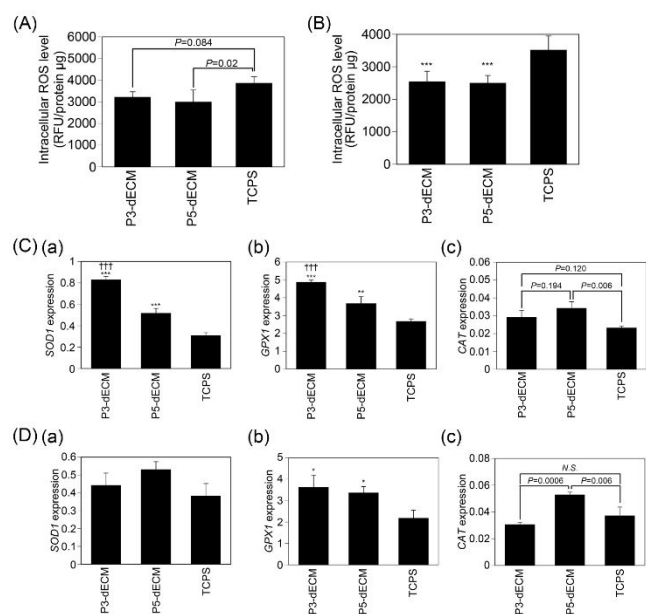


Figure 4. Antioxidant activity of NHEKs on dECM. Intracellular ROS levels in (A) P3-NHEKs under oxidative condition and (B) P5-NHEKs under normal condition. Data represent means \pm SD (n=5). ***: $P < 0.005$ vs. TCPS. (C) Gene expression levels of antioxidant enzymes, (a) *SOD1*, (b) *GPX1*, and (c) *CAT*, in P3-NHEKs under oxidative condition. (D) Gene expression levels of antioxidant enzymes, (a) *SOD1*, (b) *GPX1*, and (c) *CAT*, in P5-NHEKs under normal condition. Data represent means \pm SD (n=3). *: $P < 0.05$, ***: $P < 0.005$ vs. TCPS. †††: $P < 0.005$ vs. P5-dECM. *N.S.* indicates not significant.

P3-dECM suppressed the senescence of NHEKs during the passage culture

As demonstrated above, P3-dECM suppressed the senescence of P3-NHEKs under oxidative conditions and further progression of P5-NHEKs' senescence under normal conditions (Figure 3). Cellular senescence can be also induced by replicative stress.⁴ Therefore, I examined whether P3-NHEKs could suppress the senescence of NHEKs during passage culture. NHEKs could be passaged on P3-NHEKs, even though the yield was lower than TCPS (Table S5). NHEKs at passage two were passaged twice on P3-dECM and TCPS. The percentage of SA- β -Gal-positive cells was measured after passaged cells were cultured for 3 days on TCPS (Table 1). The percentage of SA- β -Gal-positive cells was significantly lower on P3-dECM than on TCPS. This result indicated that P3-dECM can suppress cellular senescence induced by replicative stress.

Table 1: Percentage of SA- β -Gal positive cells after the passage culture on dECM and TCPS (unit: %).

	P3-dECM	TCPS	<i>P</i> -value
#1	21.7 \pm 3.6	30.7 \pm 1.8	0.002
#2	27.1 \pm 2.2	37.4 \pm 2.2	0.00008
#3	21.8 \pm 2.8	28.7 \pm 2.1	0.002

P3-dECM increased the function of basal keratinocytes

Finally, I examined whether P3-dECM increases the function of basal keratinocytes. The gene expression levels of *AQP3*, a moisturizing molecule expressed in basal keratinocytes⁷, were measured using real-time PCR analysis (Figure 5A). *AQP3* expression levels increased by 17% on P3-dECM compared to those on TCPS. In addition, the *AQP3* gene expression is promoted by ATRA.³⁰ *AQP3* gene expression levels were measured after 3 h of ATRA exposure using real-time PCR (Figure 5B). *AQP3* expression increased by ATRA on both P3-dECM and TCPS. The response to ATRA tended to be more sensitive on P3-dECM than TCPS. These results suggest that P3-dECM can increase the function of basal keratinocytes.

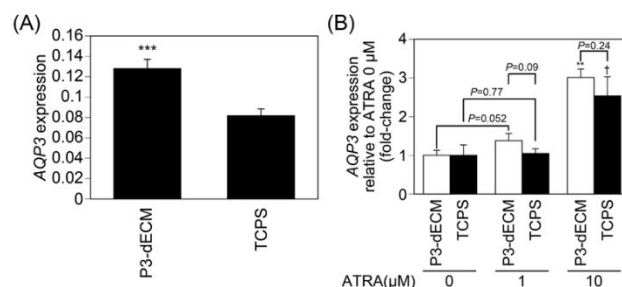


Figure 5. *AQP3* expression in P3-NHEKs on P3-dECM and TCPS. (A) Basal *AQP3* expression levels on P3-dECM and TCPS. Data represent means \pm SD (n=3). ***: $P < 0.005$ vs. TCPS. (B) Responsive ability to ATRA. Data represent means \pm SD (n=3). **: $P < 0.01$ vs. ATRA 0 μ M on P3-dECM.

Discussion

In this study, dECM were prepared by culturing P3- and P5-NHEKs at different levels of cellular senescence. Cultured NHEK-derived dECM allowed cells to adhere and grow. In particular, P3-dECM suppressed senescence of NHEK under oxidative and normal conditions and allowed NHEK passage culture with a lower induction level of cellular senescence. Oxidative stress, a stressor that induces cellular senescence, was suppressed on the NHEK-derived dECM. Finally, it was suggested that the function of basal keratinocytes increased on P3-dECM.

ECM compositions of cultured NHEK-derived dECM and cell behaviors

To compare the ECM compositions of the dECM, ECM expression patterns were compared between P3- and P5-NHEKs, and *NID-1* expression was found to be decreased in P5-NHEKs (Figure 1B). However, nidogen-1 distribution showed a similar pattern between young and aged skin.¹⁴ Moreover, *LAMA5* and *HSPG2* expression levels were similar between P3- and P5-NHEKs, although laminin α 5 chain and perlecan (heparan sulfate proteoglycan 2) decreased in aged skin.^{8, 15} The components of the basement membrane are also supplied by fibroblasts as well as keratinocytes.³¹ This is one of the reasons for the differences between *in vivo* observations at the protein level and *in vitro* gene expression. Therefore, P3- and P5-dECM

do not mimic the ECM composition of aged skin. To mimic the basement membrane more precisely, co-culture with non-senescent and senescent fibroblasts is one of the solutions to prepare dECM-mimicking native ECM.³² However, the prepared dECM suppressed senescence of NHEKs. It has been suggested that minor ECM components are effective in this suppression. Mass spectroscopy would be helpful to unveil the key ECM components to suppress senescence of NHEKs by the comparison between P3-dECM and P5-dECM.

Cell growth on NHEK-derived dECM was comparable to that on TCPS (Figure 2D, 2E, S1, and S2). However, cell adhesion was lower on the NHEK-derived dECM than on the TCPS. One possible reason is that cell adhesion-inhibiting molecules might be deposited in the NHEK-derived dECM. Tenascin-C is a matricellular protein that can inhibit keratinocyte adhesion³³, and tenascin-C is expressed by keratinocytes³⁴, which might lead to tenascin-C deposition in NHEK-derived dECM and the inhibition of NHEK adhesion. Another possible reason is that cell adhesion was not fully promoted by NHEK-derived dECM owing to insufficient deposition and assembly of ECM molecules. To improve cell adhesion, macromolecular crowders promote the deposition of ECM molecules.³⁵ Other possible reasons are not excluded at present time.

Suppression mechanisms of the senescence of NHEKs

This study demonstrated that NHEK-derived dECM can suppress senescence in NHEK cells. In particular, the suppressive effects were greater on the dECM derived from NHEKs at lower passage numbers than at higher passage numbers. It has been reported that senescence of MSCs was suppressed only on young donor MSC-derived dECM, except in aged donor MSC-derived dECM.²² Senescent cells were increased in aged tissues. Therefore, the obtained results are consistent with those of previous studies. Cellular senescence can be induced by various stressors. Oxidative stress is one of the major causes of cellular senescence.⁴ NHEK-derived dECM increased the antioxidant activity through the expression of antioxidant enzymes (Figure 4). This increase in antioxidant activity suppressed the senescence of NHEKs (Figure 3 and Table 1). However, other mechanisms cannot be excluded. For example, an increase in telomerase activity suppresses cellular senescence.⁴ Indeed, Sun et al. reported that telomerase activity increases to suppress cellular senescence on cultured MSC-derived dECM.²⁴ Mitochondrial dysfunction induces cellular senescence. SPARC modulates mitochondrial functions³⁵ and can be expressed by keratinocytes.³⁶ It is possible that SPARC deposited in NHEK-derived dECM improves mitochondrial function to suppress the senescence of NHEKs. However, other possible explanations cannot be excluded.

Antioxidant activity is a key factor in the suppression of cellular senescence. Several studies demonstrate the induction of antioxidant activity by dECM.^{21, 23, 24} This study also demonstrated that NHEK-derived dECM induces antioxidant activity. The mechanisms by which antioxidant activity promotes NHEK-derived dECM remains unclear. In this study, *SOD1*, *GPX1*, and *CAT* expression levels were measured as

representative antioxidant enzymes. Other enzymes such as SOD-2 exhibit antioxidant activity. These enzymes can also contribute to the antioxidant activity of NHEK-derived dECM.

Feasibility of P3-NHEK-derived dECM for *in vitro* 3D epidermal model development

In vitro 3D epidermal models have been frequently used for safety assessment of chemicals and efficacy testing of cosmetics.^{1, 2} However, these models impair cell viability and function after long-term culture.³ One of the reasons for this impairment is the senescence of keratinocytes.³ This study demonstrated that P3-NHEK-derived dECM suppresses keratinocyte senescence.

Epidermal stem cells (EpiSCs) are required for epidermal renewal.³⁷ Therefore, the decrease in EpiSCs is also the reason for the impairment of the epidermal models. It is unclear whether NHEK-derived dECM can maintain the stemness of EpiSCs. Several studies have reported that suppression of cellular senescence contributes to the maintenance of EpiSC populations.^{3, 38, 39} In addition, it has been reported that dECM derived from undifferentiated cells suppress spontaneous stem cell differentiation.⁴⁰ NHEK-derived dECM were prepared without induction of differentiation. Therefore, it is expected that the terminal differentiation of keratinocytes may be suppressed on the dECM. However, NHEKs are a mixture of EpiSCs and non-EpiSC-basal keratinocytes. NHEK-derived dECM are not prepared from single stem cells, which may weaken the effects of suppressing differentiation. Therefore, it is necessary to confirm whether EpiSCs are maintained on dECM.

The functions of keratinocytes are important for the development of an *in vitro* 3D epidermal model. In this study, the function of basal keratinocytes was suggested to increase on P3-NHEK-derived dECM (Figure 5). In addition to the functions of basal keratinocytes, the functions of keratinocytes in the suprabasal layers (*i.e.*, spinous layer, granular layer, and stratum corneum) should be checked after differentiation in air-liquid interface culture. In particular, dECM derived from stem cells weakens the effects of differentiation inducers.⁴¹ Therefore, an *in vitro* 3D epidermal model using P3-dECM are currently under preparation and characterization, and the results with detailed functions at protein levels will be reported in the future.

Conclusions

In this study, dECM were prepared by culturing NHEKs and decellularization. NHEKs can be cultured on these dECM with the suppression of their senescence through an increase in antioxidant activity. Senescence of NHEKs was suppressed even after passage culture. Finally, P3-dECM increased *AQP3* expression and the response to ATRA as an indicator of basal keratinocyte function. P3-dECM could be a useful cell culture substrate to prepare an *in vitro* 3D epidermal model for the safety assessment of chemicals and efficacy testing of cosmetics.

Author Contributions

T.H. conceptualized this research, designed and performed all experiments. Also, T.H. analyzed the data, acquire the funding, and wrote this manuscript.

Conflicts of interest

There are no conflicts to declare.

Acknowledgements

This work was supported by the Center of Innovation Program (JPMJCE1312) funded by the Japan Science and Technology Agency (JST), Japan, and a Grant-in-Aid for Scientific Research (C) (20K12660) funded by the Ministry of Education, Culture, Sports, Science, and Technology (MEXT), Japan.

References

- 1 A.F. Black, C. Bouez, E. Perrier, K. Schlotmann, F. Chapuis, O. Damour, *Tissue Eng.*, 2005, **5/6**, 723.
- 2 S.K. Wattanapitayakul, L. Chularojmontri, M. Schäfer-Korting, *Acta Pharm.*, 2021, **71**, 293.
- 3 M.D. Santos, E. Metral, A. Boher, P. Rousselle, A. Thepot, O. Damour, *Matrix Biol.*, 2015, **47**, 85.
- 4 V. Gorgoulis, P.D. Adams, A. Alimonti, D.C. Bennett, O. Bischof, C. Bishop, J. Campisi, M. Collado, K. Evangelou, G. Ferbeyre, J. Gil, E. Hara, V. Krizhanovsky, D. Jurk, A.B. Maier, M. Narita, L. Niedernhofer, J.F. Passos, *Cell*, 2019, **179**, 813.
- 5 Y. Wang, S. Chen, Z. Yan, M. Pei, *Cell Biosci.* **2019**, *9*, 7.
- 6 W.-L. Teng, P.-H. Huang, H.-C. Wang, C.-H. Tseng, F.-L. Yen, *Antioxidants*, 2021, **10**, 1552.
- 7 W.B. Bollag, L. Aitkens, J. White, K.A. Hyndman, *Am. J. Physiol. Cell. Physiol.*, 2020, **318**, C1144.
- 8 S. Iriyama, M. Yasuda, S. Nishikawa, E. Takai, J. Hosoi, S. Amano, *Sci. Rep.*, 2020, **10**, 12592.
- 9 B. Geiger, K.M. Yamada, *Cold Spring Harb. Perspect. Biol.*, 2011, **3**, a005033.
- 10 D. Hubmacher, S.S. Apte, *Curr. Opin. Rheumatol.* **2013**, *25*, 65.
- 11 R.O. Hynes, A. Naba, *Cold Spring Harb. Perspect. Biol.*, 2012, **4**, a004903.
- 12 R.-I. Manabe, K. Tsutsui, T. Yamada, M. Kimura, I. Nakano, C. Shimonon, N. Sanzen, Y. Furutani, T. Fukuda, Y. Oguri, K. Shimamoto, D. Kiyozumi, Y. Sato, Y. Sado, H. Senoo, S. Yamashina, S. Fukuda, J. Kawai, N. Sugiura, K. Kimata, Y. Hayashizaki, K. Sekiguchi, *Proc. Natl. Acad. Sci. U.S.A.*, 2008, **105**, 12849.
- 13 N. Levi, N. Papismadov, I. Solomonov, I. Sagi, V. Krizhanovsky, *FEBS J.*, 2020, **287**, 2636.
- 14 J. Sage, D.D. Quéral, E. Leblanc-Noblesse, R. Kurfurst, S. Schnebert, E. Perrier, C. Nizard, G. Lalmanach, F. Lecaille, *Matrix Biol.*, 2014, **33**, 41.
- 15 M.D. Santos, A. Michopoulou, V. André-Frei, S. Boulesteix, C. Guicher, G. Dayan, J. Whitelock, O. Damour, P. Rousselle, *Aging*, 2016, **8**, 751.
- 16 N. Nakamura, T. Kimura, A. Kishida, *ACS Biomater. Sci. Eng.*, 2017, **3**, 1236.
- 17 A. Costa, J.D. Naranjo, R. Londono, S.F. Badylak, *Cold Spring Harb. Perspect. Biol.*, 2017, **7**, a025676.
- 18 T. Hoshiba, *J. Mater. Chem. B*, 2017, **5**, 4322.
- 19 T. Hoshiba, T. Yamada, H. Lu, N. Kawazoe, G. Chen, *J. Biomed. Mater. Res. A*, 2012, **100**, 694.
- 20 T. Hosokawa, T. Betsuyaku, M. Nishimura, A. Furuyama, K. Katagiri, K. Mochitate, *Connect. Tissue Res.*, 2007, **48**, 9.
- 21 Y. Lai, Y. Sun, C.M. Skinner, E.L. Son, Z. Lu, R.S. Tuan, R.L. Jilka, J. Ling, X.-D. Chen, *Stem Cells Dev.*, 2010, **19**, 1095.
- 22 J. Li, K.C. Hansen, Y. Zhang, C. Dong, C.Z. Dinu, M. Dzieciatkowska, M. Pei, *Biomaterials*, 2014, **35**, 642.
- 23 X. Liu, L. Zhou, X. Chen, T. Liu, G. pan, W. Cui, M. Li, Z.-P. Luo, M. Pei, H. Yang, Y. Gong, F. He, *Mater. Sci. Eng. C Mater. Biol. Appl.*, 2016, **61**, 437.
- 24 Y. Sun, W. Li, Z. Lu, R. Chen, J. Ling, Q. Ran, R.L. Jilka, X.-D. Chen, *FASEB J.*, 2011, **25**, 1474.
- 25 M.M. Movahednia, F.K. Kidwai, Y. Zou, J.J. Tong, X. Liu, I. Islam, W.S. Toh, M. Raghunath, T. Cao, *Tissue Eng. Part A*, 2015, **21**, 1432.
- 26 T. Hoshiba, *Curr. Protoc.*, 2021, **1**, e318.
- 27 T. Hoshiba, S. Yunoki, *J. Biomed. Mater. Res. B*, in press, <https://doi.org/10.1002/jbm.b.35135>.
- 28 T. Kuilman, C. Michaloglou, W.J. Mooi, D.S. Peeper, *Genes Dev.*, 2010, **24**, 2463.
- 29 E.J. O'Keefe, D. Woodley, G. Castillo, N. Russell, R.E. Payne Jr., *J. Invest. Dermatol.*, 1984, **82**, 150.
- 30 G. Bellemère, O. Von Stetten, T. Oddos, *J. Invest. Dermatol.*, 2008, **128**, 542.
- 31 R. Fleischmajer, A. Utani, E.D. MacDonald II, J.S. Perlish, T.-C. pan, M.-L. Chu, M. Nomizu, Y. Ninomiya, Y. Yamada, *J. Cell Sci.*, 1998, **111**, 1929.
- 32 A. Furuyama, K. Kimata, K. Mochitate, *Cell Struct. Funct.*, 1997, **22**, 603.
- 33 M. Latijnhouwers, M. Bergers, M. Ponc, H. Dijkman, M. Andriessen, J. Schalkwijk, *J. Invest. Dermatol.*, 1997, **108**, 776.
- 34 A.G. Abdou, A.H. Maraee, M.A.E. Shoeib, R. Elbana, *Appl. Immunohistochem. Mol. Morphol.*, 2012, **20**, 501.
- 35 A. Melouane, M. Yoshioka, J. St-Amand, *Mitochondrion*, 2020, **50**, 63.
- 36 W.R. Swindell, K. Bojanowski, R.K. Chaudhuri, *J. Invest. Dermatol.*, 2020, **140**, 602.
- 37 N. Liu, H. Matsumura, T. Kato, S. Ichinose, A. Tanaka, T. Namiki, K. Asakawa, H. Morinaga, Y. Mohri, A. De Arcangelis, E. Geroges-Labouesse, D. Nanba, E.K. Nishimura, *Nature*, 2019, **568**, 344.
- 38 C.L. Tan, T. Chin, C.Y.R. Tan, H.A. Rovito, L.S. Quek, J.E. Oblong, S. Bellanger, *J. Invest. Dermatol.*, 2019, **139**, 1638.
- 39 A. Giangreco, S.J. Goldie, V. Failla, G. Saintigny, F.M. Watt, *J. Invest. Dermatol.*, 2010, **130**, 604.
- 40 X.-D. Chen, V. Dusevich, J.Q. Feng, S.C. Manolagas, R.L. Jilka, *J. Bone Miner. Res.*, 2007, **22**, 1943.
- 41 T. Hoshiba, N. Kawazoe, T. Tateishi, G. Chen, *J. Biol. Chem.*, 2009, **284**, 31164.